Final Project Report

Cathode Blades: Hadrian Sneed, Stephen Klem, Henry Nester, & Nathan Hersel

CONTENTS

I. STATEMENT OF WORK

Hadrian I was responsible for the basic idea of this project, part orders, and creating the pcb layout in Kicad. The layout I created went through many design changes in an iterative process that relied heavily on the feedback from Henry. Not all part orders were done by me, and most of the electrical components were ordered by Henry. I was also responsible for creating the assembly drawing of the mechanical design and the part drawing for the tool holder, which was machined for me by Mr. Sebring Smith, the shop manager at Lacy Hall.

Stephen I was in charge of select responsibilities for the group. At the start, I researched and selected the aquatic pump for our dielectric pump-system. Furthermore, I created the foundational form of the pumping component-sector's block diagram. Then, I

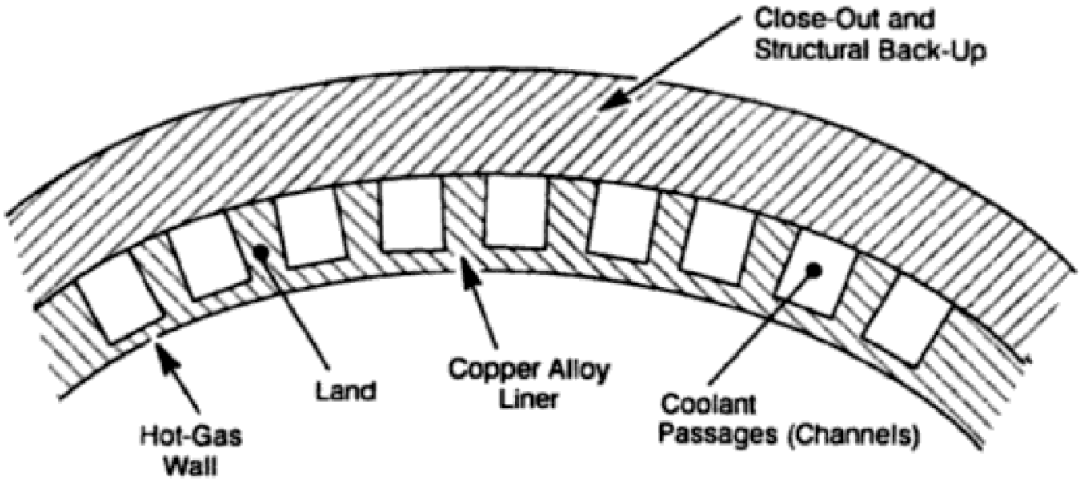

Fig. 1: Typical channel-wall configuration using regenerative cooling method two [2]

handled the seeking and acquisition of a power supply here on Grounds. After this, I helped formulate the objectives, areas, and initial methods for preliminary testing. I then coordinated externally with UVA's Environmental Health and Safety (EHS) Department, in order to arrange for the group to undergo high-voltage safety training that was required for our project. Throughout this task, I relayed necessary technical information and documents between group members and the corresponding EHS supervisor. When the group was conducting operational and performance testing, I was in charge of observing that proper safety protocols were in practice. Finally, I produced and edited the video that represents our group's Capstone project for this semester.

Henry I was responsible for the project feasibility physics calculations in the early project stages and took on the circuit design later in the project. I researched parts and circuit topologies, then entered the schematic into KiCAD, including finding or making footprints for all parts. I made 10 mistakes in the schematic design, mostly for lack of attention to detail, but was luckily able to understand each issue and greenwire a fix on the PCB. I also helped Nathan by writing the parts of the firmware that configured the microcontroller peripherals to operate as part of the circuit.

Nathan I was tasked with setting up and working with the embedded code throughout the project phases. I began this project by learning how to use the STM32 microcontroller and setting up the code for the stepper motor. Next, I worked with Henry to set up the various microcontroller peripherals. Once the peripherals were setup, I worked on implementing a finite state machine for the project. Throughout the project, I worked a lot with Henry to get the code performing as required and at the end of the project we debugged the code by adjusting different parameters so that the device would operate as intended.

II. Abstract

Our project seeks to develop a better process for manufacturing regenerative cooling channels. Regenerative cooling is used in reusable rocket engines to redirect the extremely high heat flux resulting from combustion. Our process will use an electrical discharge machining (EDM) device to erode thin channels into a single solid workpiece. EDM uses arcing resulting from the cold emission of electrons in a strong electric field. The ions generated from this arcing, which usually propagates in a dielectric, rapidly heat a microscopic section of the workpiece and causes that section to sublimate and erode from the bulk of the material. This arcing process is repeated many times a second to erode the desired shape from the workpiece. [1]

III. Background

Regenerative cooling follows one of two designs. The first and older method uses tightly packed tubes that flow coolant through the walls of the combustion chamber. [3] The second method is to carve channels into the inner wall of the engine and use electrodeposition to create the outer wall or "close-out" of the engine to enclose the channels for coolant to run through them. Fig. 1 shows a typical cross-section of a channel wall that uses this method of regenerative cooling. Today, this method is largely favored since it allows for thicker walls to "permit 'smoothing' of any localized extremely-high-heat-flux regions" and it allows the use of "high conductivity materials for wall construction". [2] Because of these advantages. This project will focus on machining regenerative cooling channels similar to the second method.

Our group chose EDM as an alternative manufacturing process for channel-wall regenerative cooling for two reasons. First, EDM allows us to carve extremely long, thin, and precise channels out of a single workpiece. Also, EDM does not cause significant changes to the mechanical properties of the workpiece during machining nor will it introduce any new stresses. [1] The EDM device we design will be similar to a type of EDM called die-sink EDM. This type of EDM is characterized by having the workpiece submerged in flowing dielectric and the tool is lowered slowly into the workpiece until the desired shape is eroded. This is in contrast to wire EDM where the tool is a spool of thin conductive wire with dielectric flowing along its length and dry EDM, which is similar to

die sink EDM but uses no dielectric. [1] Other more niche types of EDM exist like micro EDM for smoothing surfaces and hybrid EDM.

Die-sink EDM is the best choice for our project for a number of reasons. Wire EDM cannot make holes directly in the workpiece and would require a starter hole to create the channels needed for regenerative cooling in a single solid workpiece. Requireing starter holes that stretch all the way through the workpiece defeats the purpose of such a device for this application. Micro EDM is not designed for removing large amounts of material and the time needed to do so would be completely prohibitive. Dry EDM struggles to remove or flush the sublimated workpiece material making such a system unstable for the purposes of eroding thin channels. Electrical Discharge Hybrid Machining systems require the use of multiple electrical or electrochemical machining processes, which is needlessly complicated for our purposes. In summary, die-sink EDM offers us advantages in simplicity, speed, and reliability over other types of EDM.

The system we have designed incorporates our understanding of: basic circuitry from the Fundamentals courses, transistor operation from Solid State Devices, micro-controller programming from Embedded Computer Systems, and electric fields across a dielectric from Electricity and Magnetism.

IV. Societal Impact Constraints

There are two main stakeholders to consider regarding this project Machinists using the EDM device and untrained persons near the device. For the first stakeholder, trained machinists, training in other machining or cnc devices does not qualify them to use our EDM device. This is true for two reasons. First, the use of our EDM device is significantly different from the use of manual machining devices and most CNC devices. Second, EDM presents unique safety considerations. For these reasons, machinists must be trained in EDM machining in order to be qualified to use our device.

The second stakeholder are untrained people who may interact with the EDM device. Since these people are not qualified to use the device, they should not touch any part of the device including the laptop controlling it from a distance. Touching high voltage elements of the device risks nonlethal shocks that can cause burns and muscle contractions. Though the voltages used in this device do not meet the UVA EH&S qualifications for high voltage DC, our group thought it prudent to erect a barrier one foot from the device to prevent unsafe interaction as is recommended for voltages slightly higher than ours. At the outset of this project, it was suspected that the sparking process would release ultraviolet light with enough flux to damage retinas if eye protection is not worn. After constructing the device, it was determined that this is not the case and the device presents little risk of eye damage. Still, as a precautionary measure, the sparks will be behind the walls to the tub used to contain the dielectric and should not be visible.

V. Physical Constraints

A. Costs

This project was given a budget of $500 by the University of Virginia. We exceeded this budget and covered the remaining costs by paying for them from our own funds. The budgetary constraints of this project limited us in the parts that we could use to create our device. A traditional tool holder and EDM tool would cost hundreds of dollars and we needed to machine or own tool holder and use simple copper rods as our tool. We were also limited in our flushing system as we were unable to afford a filter to remove sublimated particulates from the work-piece out of our deionized water. Without being able to afford a traditional edm tool, we were unable to pump water out of the end of our tool, which also limited flushing. Finally, we were only able to use aluminum as a workpiece for testing since we were unable to afford any other materials. See the Costs section and table I for more detailed accounting.

B. Design and Manufacturing

The main manufacturing constraint to this project was the inability for our pcb to be ordered through the class Advanced Circuits ordering process. Namely, the program used to panelize the pcbs for our class was unable to load our board's gerber files despite them passing dfm tests. After troubleshooting with the help of the professor, the problem could not be resolved and our group was forced to order our board through JLCPCB instead. This also limited the time we had to solder components and test the board once it arrived. Also, because of time constraints, parts that were needed towards the end of this project were ordered from Amazon using Amazon Prime at our group member's personal expense.

C. Tools

The tools used in this project were:

- Autodesk Inventor Professional 2023
- Waterjet CNC machine
- KiCad
- Soldering Iron
- Multimeter
- Oscilloscope
- Wire clippers
- Wire strippers

- Laptop
- GNU ARM Embedded Cross-compiler for x86-64 architecture and associated linker and binary utilities
- GNU Debugger (gdb) server

VI. External Standards

Based on FCC standard 15.101, because the EDM device operates below 30 MHz, it is exempt from this section, but must still follow standard 15.5. Standard 15.5 states general conditions of operation. This standard discusses that operation of the device is subject to the conditions that no harmful interference is caused and the operator must cease operating the device when notified by a commission representative. [14] [15] This was was considered while performing testing and setup. UVA Health and Safety standards require that anything greater than 100 VDC must follow special safety procedures when testing equipment. Because the project did not exceed 100 VDC, these safety procedures were not required. However, all members of the team did participate in high voltage safety training in case that the project happened to go over 100 VDC. [16] The safety training discussed how to properly setup a workspace, prevent others from being harmed by the project, as well as other general safety concerns. IPC standards were followed for component sizes when designing the PCB. IPC standards 7351 ensures that the correct footprint sizes will be used. [17] IPC-2221 was followed to guarantee the correct trace spacing when designing the PCB. [18]

VII. Intellectual Property Issues

Patent number JP6140228B2 is an EDM device that controls the machining conditions of the device. This patent uses machine learning to get the machining conditions more correct. The conditions that the device controls includes the power supply voltage and the machining fluid. [19] The difference from this patent and the project being designed is that the current project does not use any machine learning to adjust the machining conditions. US patent number US9707637B2 patents the EDM process that includes the vibratory movement to allow the liquid dielectric to wash out debris. [20] However, this patent uses a high pressure pump to flow the dielectric, which is something that this project does not do. US patnet US20200238414A1 is an EDM device that has a robotic arm that can move in six different directions instead of the two that this project is using. [21]

Regardless of these patents, the current project has some unique characteristics that sets it apart from each of these three. This project does not include the extra features that the three above have. Because this project is meant to be a small scale EDM device, it is different from other patents in that it is currently meant only to drill holes through metal. While the other patents are all able to drill holes through a piece of metal, this project uses a more simple approach and encompasses the whole setup. The patent for this device would include a tub that the mechanical portion and a water pump sits in so that the work piece is covered in dielectric. The other patents focused on the mechanical device and not the entire setup of the project. If a patent were to be sought after for this project, an independent claim would be filed because this project is too different from other patents to add on to another one. This design allows for a relatively low cost option to a traditionally expensive process.

VIII. Project Description

A. Software design

The embedded part of the project was done by using several different peripherals to be able to use the microcontroller to control the outputs, detect inputs, and to communicate between the computer and the microcontroller. After the peripherals were setup, a state machine was developed for the device to run automatically with limited user input. The FSM diagram is shown in figure 2 and the peripheral diagram is shown in figure 3. The state machine works by beginning in the stop state and moving to the up state if the 'u' character was sent over USART or moving to the down state if the 'd' character was sent. This made it possible for the tool piece to be positioned easily. Also while in the stop state, if the 'r' character was sent, the state machine moves into the pre-charge state where it waits for a short period of time and then moves into the run state. It stays in this state until the 's' character is received or until the Analog Watchdog is triggered because a short was detected. While in the run state, the timer peripherals control how long the spark is left on. Looking at figure 3, the spark detect triggers TIM1 to turn on and after an amount of time, the spark switch turns on. After another amount of time following the spark switch, the ADC is triggered and reads the voltage coming in from the device. The AWD is triggered if a short circuit is detected and then moves the FSM into the stop state.

B. Schematic design

The electrical schematics for this project are shown in Fig. 4, 5, 6, 7, 8 were developed to satisfy the project requirements via an iterative process. See the figure captions for an explanation of how each subsystem works.

C. PCB design

The PCB was modeled using kicad. The final design for the pcb can be seen in figure 9. In this and the following layouts, red lines and planes represent top copper layer traces and blue represents bottom copper layer traces. Bright yellow elements are painted onto the silkscreen layer. Grey elements are just for our reference in the cad layout and not present on the final board.

In figure 10, we see a closer look at the high voltage elements of the pcb. Note that because of the high currents involved, high voltage nodes are mostly large fill zones. The resistors used in the adc voltage sensor and spark detection comparator (R17 and R16)

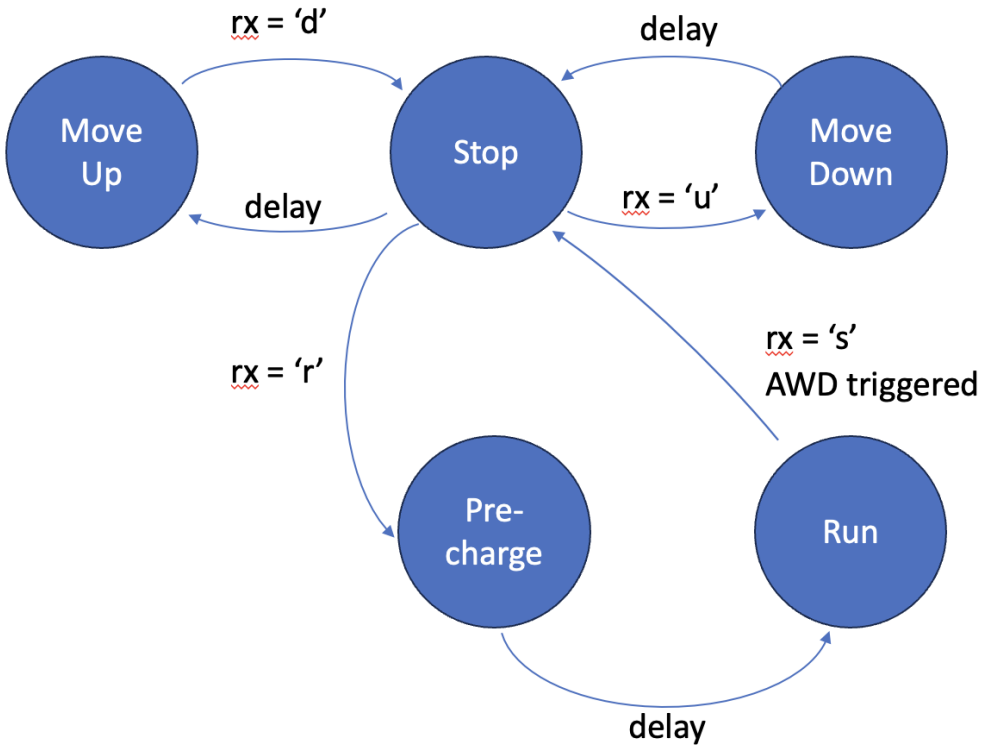

Fig. 2: Diagram of Finite State Machine

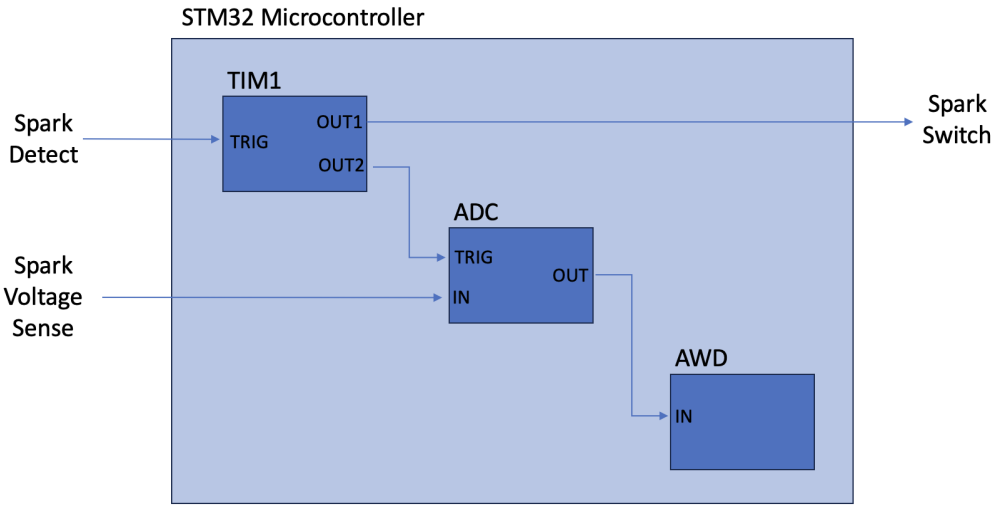

Fig. 3: Diagram of Peripheral Setup

can be seen on the left. The relay (K1) is the mechanical high voltage shutoff that flip in the event of short circuit detection. The MOSFETs (Q1-4) that are turned on to trigger a spark can be seen on the left.

In figure 11, we can see the BJTs (Q6-10) that drive the high voltage MOSFETs. After attempting to implement the design, it was determined that this driver design did not function and the PNP BJTs (Q7 and Q9) were removed and R22 was shorted to R23 to resolve this issue.

Figure 12 shows the layout for the STM32 micro-controller. Due to inductance on the UART pins, the STM32 was removed from the board and the necessary pins were wired to an external secondary micro-controller.

D. Specifications and objectives

The core objective of this project is to make thin channels all the way through a thick aluminum workpiece. The qualities that our end user will desire for our EDM device are: the speed of workpiece erosion, an easy to use interface, clear display of relevant parameters, safety, and the precision of the finished holes. The speed of workpiece erosion will be measured by the Material Removal Rate (MRR) in mm^3 per minute. The MMR may depend upon the material being machined, but due to the financial constraints of

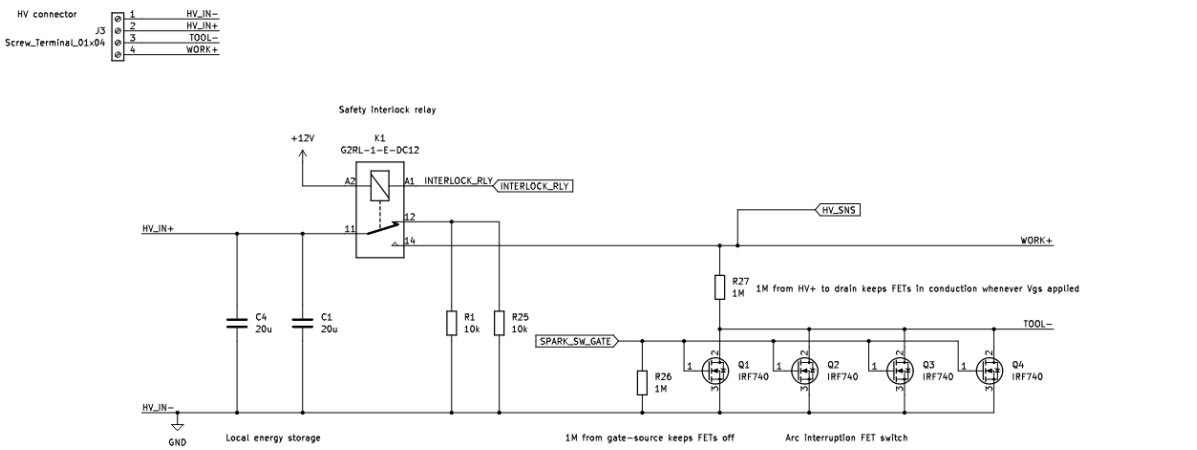

Fig. 4: High-voltage subsystem schematic. A safety interlock relay (K1) discharges the spark capacitor bank (C1 and C4) through resistors unless its coil is energized, in which case it supplies power to the spark gap. Four paralleled n-channel MOSFETs (Q1-Q4) form a high-speed solid-state switch for spark timing control, and are held in slight conduction even when the plasma channel is not present by a shunt resistor (R27) to maintain the gap field.

this project, we will be testing the MMR for aluminum. We can easily evaluate this by dividing the total volume of a finished hole by the time it required to machine.

The ease of use and clarity of information will be ensured by including a clear user interface through a USB connection between a laptop and our micro-controller. Our design will promote safety with clear labeling of high voltage surfaces and by complying with relevant IEEE and UVA safety standards. Finally, we can measure the precision of our machining by precisely measuring the difference in the diameter of our tool versus the diameter of our hole with calipers. We expect to be within $50 \pm 5\mu\text{m}$ of the tool diameter.

E. Theory of operation

Fig. 13 shows the principal subsystems in our EDM system and how they work together. There are four principal parts of the system: the machining assembly (far right, including the electrodes and provisions for moving them and pumping dielectric), the EDM control box (center, including the control electronics for the process), the high-voltage power supply (a commercial unit we will not design), and the user interface running on a control laptop. Most of our design effort will focus on the EDM control box and the machining assembly.

The microcontroller has two main roles in order to ensure the cut proceeds smoothly. First, it adjusts the z-axis height continuously to regulate the gap distance as material is removed. If the average gap voltage (as measured using an ADC) is too low, indicating a short, the tool should move up; if the gap voltage is too high, indicating an open, the tool should move down. When this voltage is in the appropriate range, sparks occur reliably each time the tools is energized. Second, it controls the timing of voltage pulses to the tool to ensure that sparks are neither too brief (which would lead to a very slow cut) nor too lengthy (which could lead to a welding of the tool to the workpiece, ruining the part). At a set interval, the tool is energized by closing the arc interruption switch. After a variable time, the gap will break down and start to conduct, dropping the gap voltage. This triggers a timer for a few microseconds in the microcontroller; when it elapses, the arc interruption switch opens again to extinguish the spark. The cycle repeats thousands of times each second to slowly erode material.

The microcontroller also has a few auxiliary tasks. It controls the safety interlock, which can deenergize the tool electrode and capacitor, if an error is detected or the user requests an emergency stop. It also communicates over an electrically isolated serial port with a UI running on the laptop to allow the operator to monitor and control the process.

The power architecture is fairly simple. Most of the system is referenced to the high-voltage (100V) power supply ground. A 12V step-down switching regulator efficiently generates power for the interlock and interruption switch gates and the stepper motor driver.

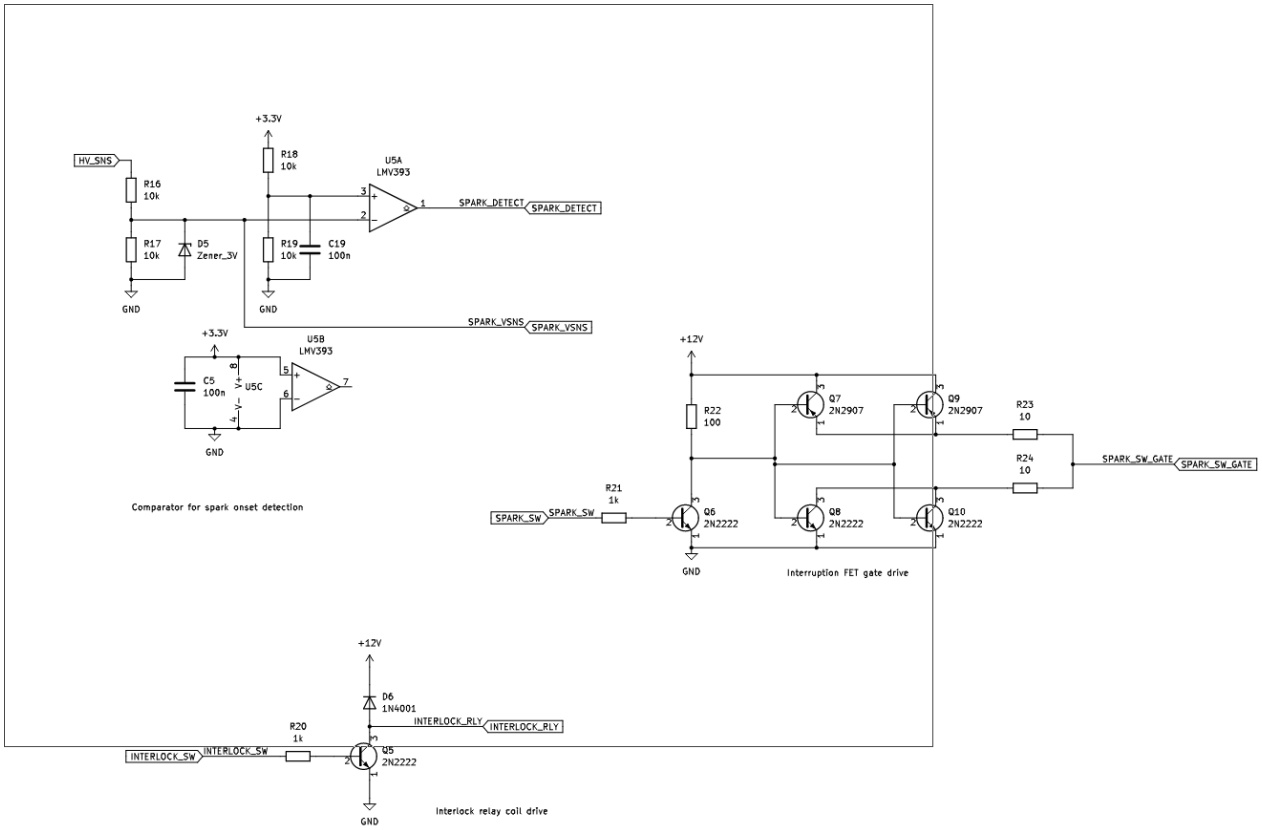

Fig. 5: High-voltage control and monitoring subsystem schematic. A Zener-clamped 50:1 voltage divider circuit (R16 and R17) scales the high-voltage level down within the logic rail (3.3V) for a microcontroller ADC input to measure. A high-speed open-drain comparator (U5A) is configured to bring a microcontroller capture-compare input LOW as soon as a spark makes the gap voltage fall. A BJT-based gate driver circuit consisting of a level shifter (Q6) cascaded with a dual push-pull driver (Q7-10) amplifies a 3.3V output to drive the gates of the spark switch MOSFETs with a fast-edged 12V signal. A low-side BJT switch (Q5) drives the interlock coil, shunted by a flyback diode so that back EMFs don't damage Q5.

A 3.3V linear regulator reduces the 12V rail to supply the microcontroller. The USB-serial converter is powered from a USB port connected to a laptop and optically isolated from the rest of the system to protect the operator from high voltages.

F. Feasibility analysis

1) Achieving dielectric breakdown: For the EDM system to work at all, the gap between the tool (cathode) and workpiece (anode) electrodes must reliably sustain sparks when a voltage is applied. When the electric field exceeds some critical strength, a spark becomes inevitable - our task is to calculate this critical field strength $E*$. In the parallel-plate limit appropriate here, the field depends on the voltage V and gap distance d

$$E = V/d$$

We would prefer to use lower voltage (below 1kV) to avoid the difficulty of producing, switching, and measuring high voltages. Reducing the gap distance can of course make E arbitrarily large without requiring a high voltage, but tiny gaps require high z-axis resolution to maintain the gap as the tool moves down into the cut. The best z-axis resolution we can hope to achieve is similar to what a typical 3D printer does: around 2.5um, driving a minimum gap of 25um. Thus the strongest field we can reasonably achieve is $E = 100\mathrm{V}/25\mu\mathrm{m} = 4\mathrm{MV/m}$.

A series of physical processes conspire to lower the critical field strength from that indicated by the intrinsic dielectric strength of water (65MV/m). Observations of EDM machines show that breakdown often occurs starting from micron-scale gas bubbles on the cathode [8]. The mechanism is not officially understood, but a literature review suggests a multi-step breakdown process. First, a current density near $10^4\mathrm{A/m}^2$ near the cathode splits the water into hydroxide ions and hydrogen gas, and bubbles of hydrogen and water vapor form, a few microns in size [7]. To verify that we can reach this critical current density in the dielectric fluid, we can compute (using a resistivity of $\rho = 10^3\Omega\mathrm{m}$, between the 10^2 for tap water and 10^5 for pure water)

$$J = \frac{V}{RA} = \frac{V}{\rho d} = \frac{100\mathrm{V}}{10^3\Omega\mathrm{m} * 25\mu\mathrm{m}} = 4000\mathrm{A/m}^2,$$

a bit short of the mark. However, the current does not distribute uniformly over the cathode surface, concentrating on microscopic sharp points [7], giving us some margin for error.

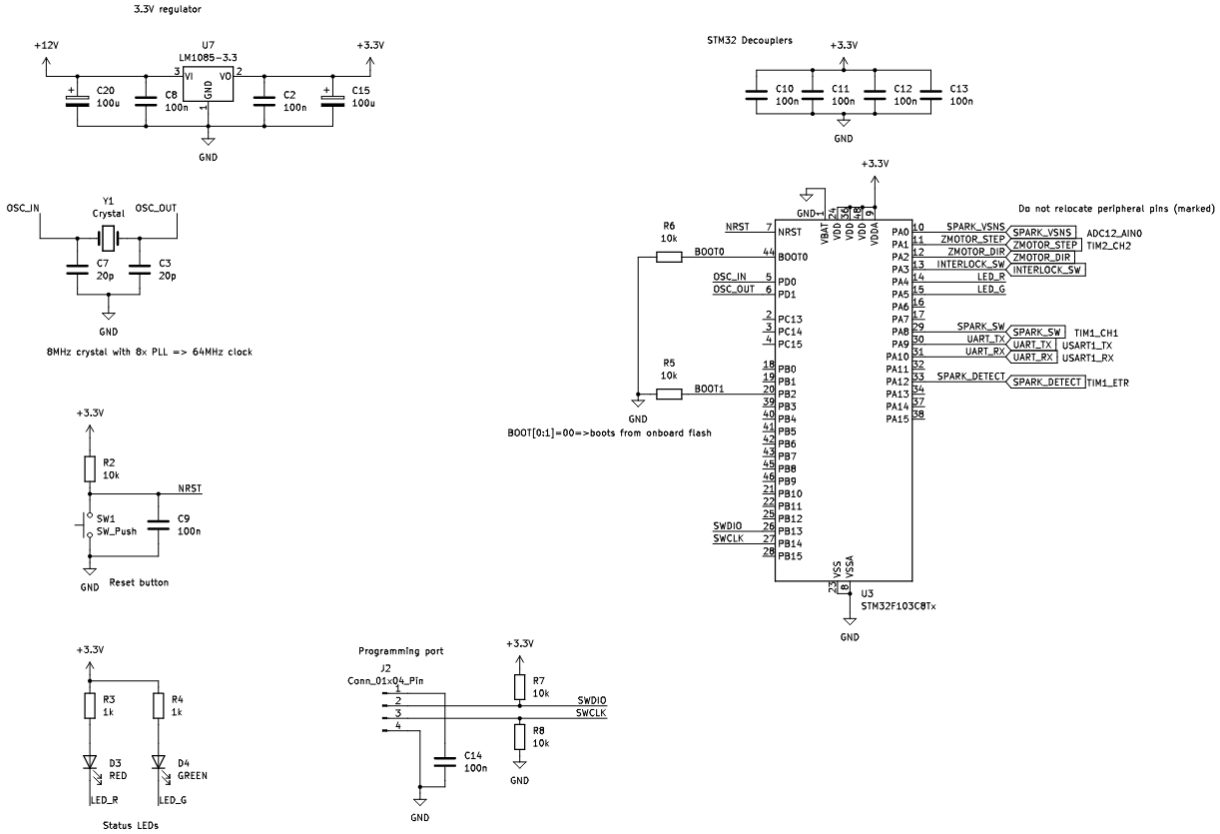

Fig. 6: Microcontroller subsystem schematic. A 3.3V linear regulator (U7) decoupled by capacitors powers an STM32F103C8T6 microcontroller running on an external 8MHz crystal (Y1). Debug LEDs, a programming port, and a reset button are all included.

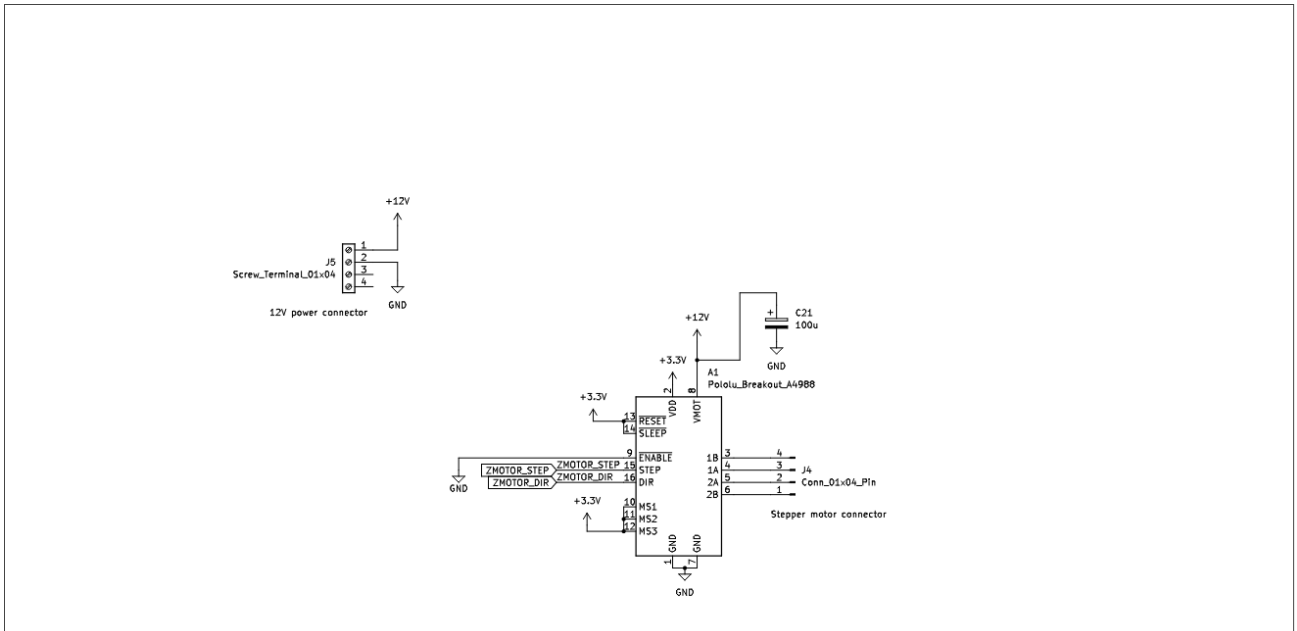

Fig. 7: Z-axis motor driver subsystem schematic. An A4988 motor driver breakout is wired to control the two-coil stepper motor in sixteenth-microstepping mode.

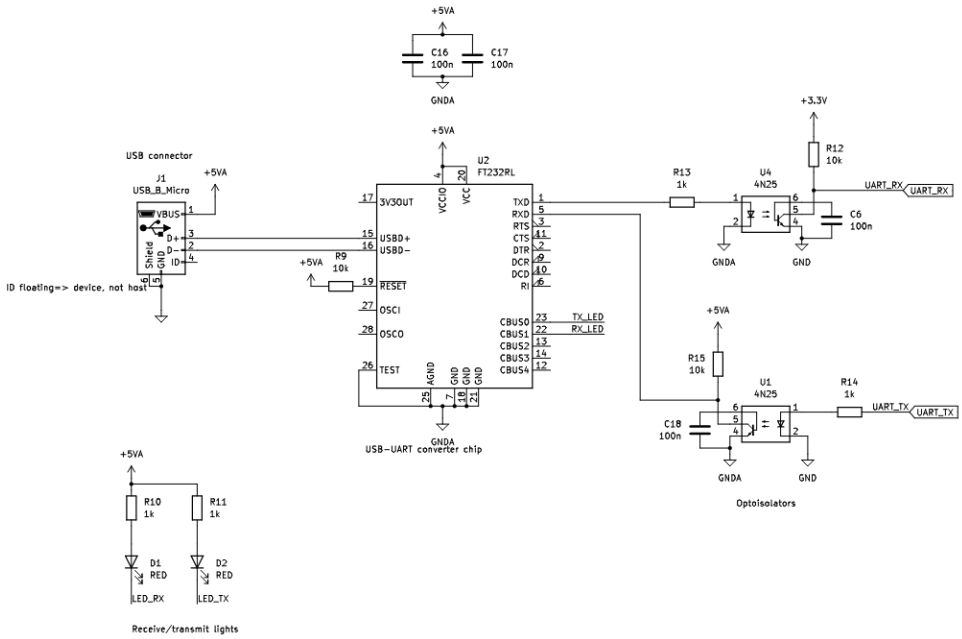

Fig. 8: A micro-USB port is wired to an FTDI USB-UART converter which interfaces to the microcontroller via a pair of unidirectional optocouplers. This subsystem is entirely powered via the USB port so that high-voltages entering the microcontroller's logic domain cannot propagate back to the control PC and its human.

The next step in breakdown involves elongation of these bubbles to bridge the electrodes. Ordinarily, the balance between surface tension and gas pressure leads to spherical bubbles, but in an electric field, the bubble elongates slightly in the field direction [10]. The differential permeability strengthens the field inside the bubble by a factor 1.5 to 6MV/m, strong enough that the number of gas ions will increase exponentially by Townsend's mechanism [9]. The bubble then behaves like a conductor, with an effective $\epsilon \to \infty$, in which case the bubble can elongate much more. At a critical electric field, the equilibrium vanishes and the bubble elongates indefinitely [10], bridging the two electrodes to initiate a spark. To compute this critical field we plot the elongation γ (major-minor axis ratio) of the bubble with respect to the applied field E according to the complicated function derived in [10] to find that $E* = 1.6\mathrm{MV/m}$ (Fig. 14). Thus our 4MV/m field is strong enough to destabilize any bubbles that form.

Now that the bubble of plasma connects the two electrodes, plenty of current will flow, ionizing more gas [4]. If the current is not interrupted, a destructive arc will form.

2) Resolution of the z-axis actuator: As mentioned above, to maintain a gap d, we require a z-axis actuator resolution near $d/10$, or $2.5\mu\mathrm{m}$. Using a stepper motor with step angle $\Delta\theta$, microstepping level m, and lead screw pitch t, the resolution will be

$$\Delta z = \frac{\Delta\theta}{360^\circ}\frac{1}{m}t$$

or for a NEMA-17 stepper motor with $\Delta\theta = 1.8^\circ$, an A4988 stepper driver with maximum microstepping $m = 16$, and a typical T8 lead screw with pitch $t = 2\mathrm{mm}$, we find $\Delta z = 0.6\mu\mathrm{m}$. Of course, the actual position will be less precisely adjustable due to vibrations in the structure and so forth, but this suggests we can achieve good-enough precision in the tool's motion to perform a cut.

3) Energy source for the spark: The spark consumes a large quantity of electrical energy in a very brief time, more than the power supply can deliver, so we intend to place a capacitor bank near the spark gap as local energy storage. A typical EDM machine creates sparks of current 250A or lower and duration 5µs or shorter [5]. The spark burn voltage is around 20V according to [5], much lower than the voltage required to initiate the spark. To give some margin for error, we set the minimum capacitor voltage to 50V and compute the size of the bank as

$$C = \frac{I_{spark}t_{spark}}{V_0 - V_{min}} = \frac{250\mathrm{A} * 5\mu\mathrm{s}}{100 - 50\mathrm{V}} = 25\mu\mathrm{F}$$

which is not unreasonable to achieve. Research suggests that a metallized polypropylene film capacitor would work well for this application, because of the high discharge current capability without damage to the capacitor's metal films, and also because of the reasonably high breakdown voltage of these capacitors [11].

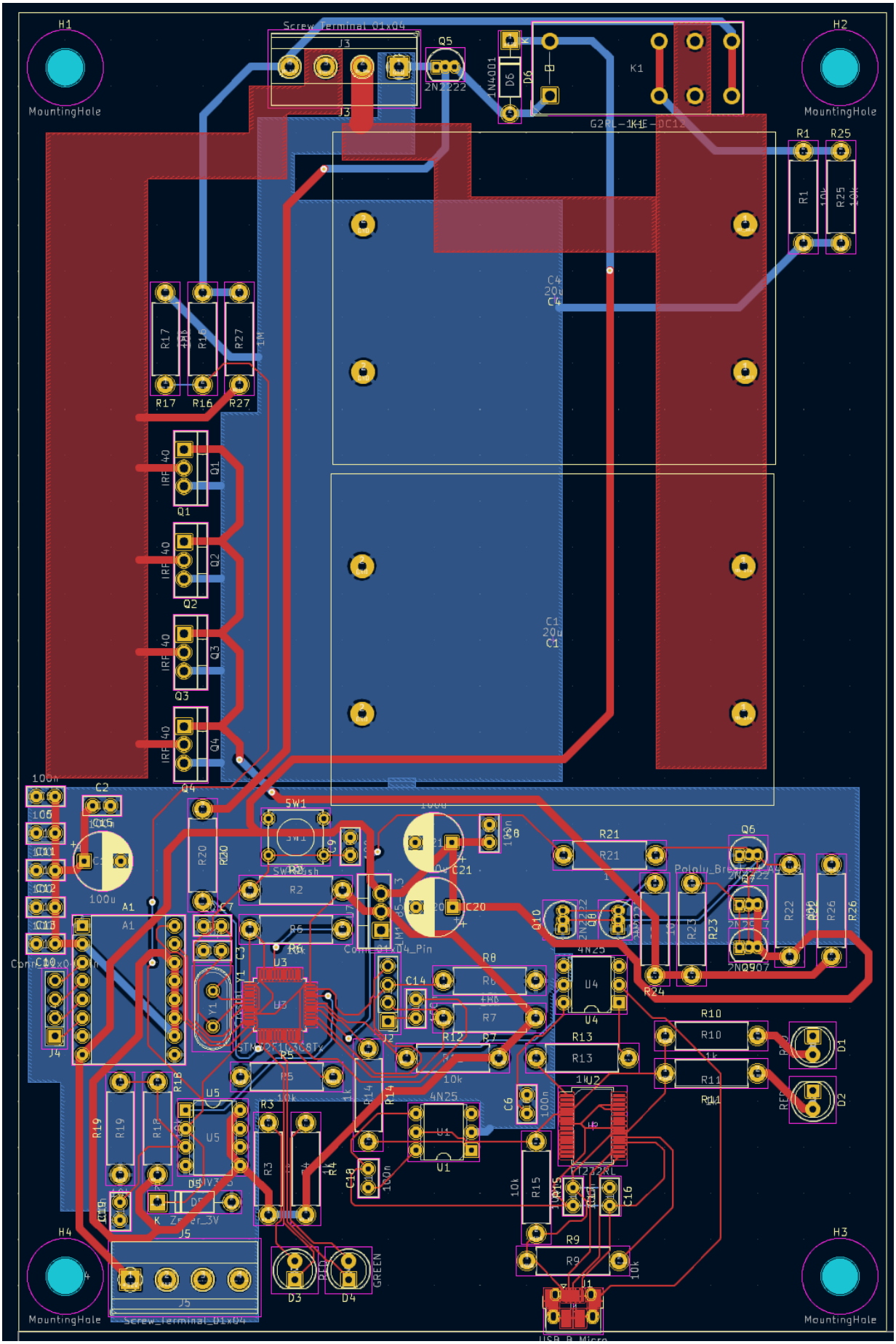

Fig. 9: Final layout of the final pcb design in kicad. Red lines and planes represent top copper layer traces and blue represents bottom copper layer traces. Bright yellow elements are painted onto the silkscreen layer. Grey elements are just for our reference in the cad layout and not present on the final board.

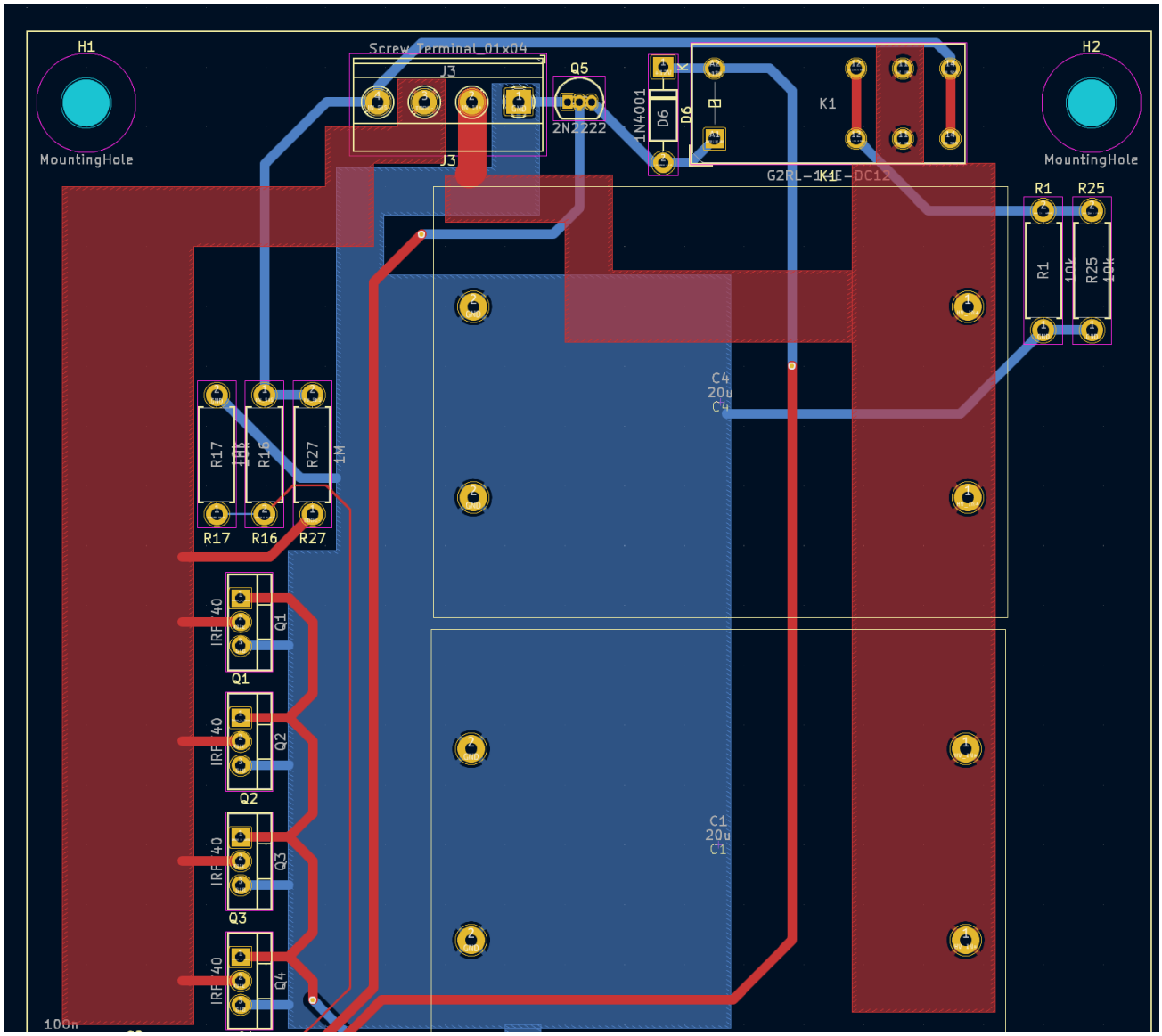

Fig. 10: Close look at the high voltage elements of the pcb. See figure 9 for color code.

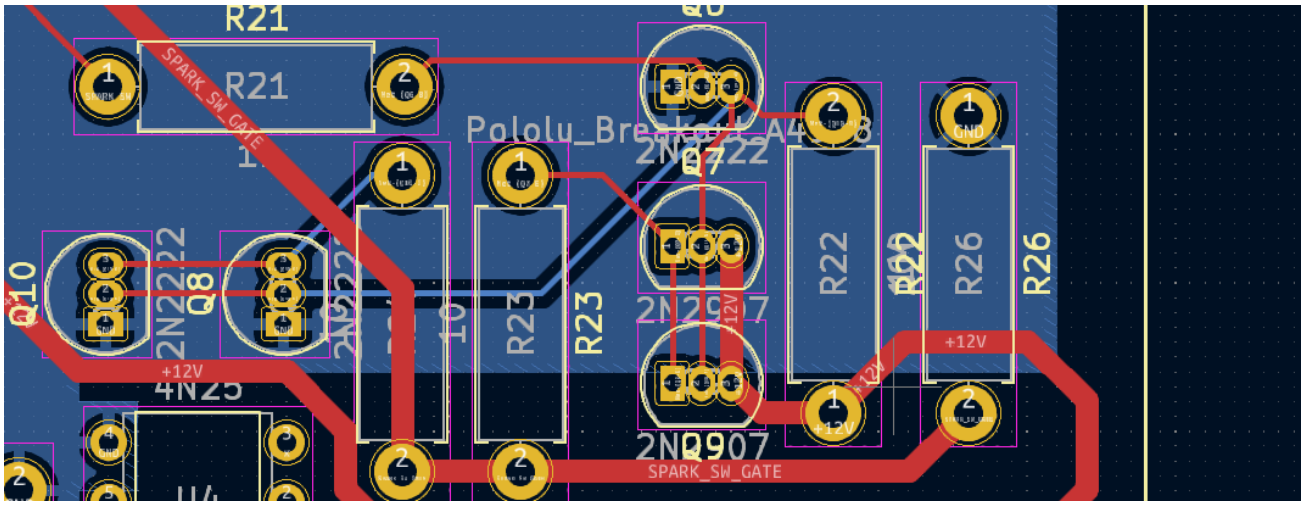

Fig. 11: Close look at the BJTs that drive the MOSFETs in the pcb. See figure 9 for color code.

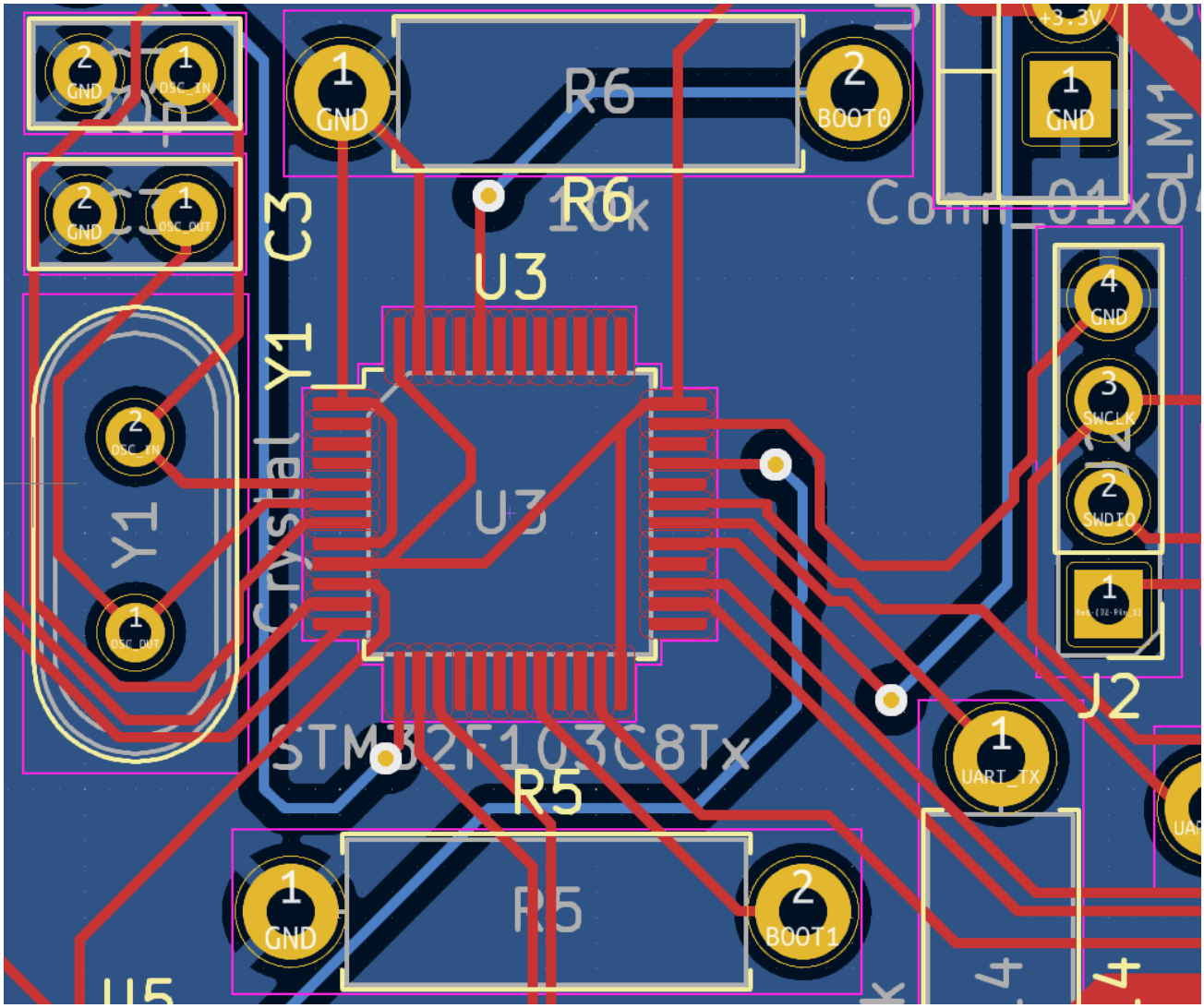

Fig. 12: Close look at the BJTs that drive the MOSFETs in the pcb. See figure 9 for color code.

The pulse discharge capability of a capacitor is typically captured in a voltage slew rating and a maximum current rating. For the 10µF Kemet capacitor that looks most promising, these ratings are $100\mathrm{V}/\mu\mathrm{s}$ and $1kA$ [12], which certainly meet our requirements. Most of these capacitors are not rated for ESR and ESL, which will effect the dynamics of the spark startup. We found several polypropylene film capacitors which meet our specifications and will switch them in and out of our prototype apparatus to determine the best choice.

4) Precision timing of the spark: Another difficulty with this project is the precise regulation of the spark duration. The spark does not start up immediately when voltage is applied to the gap: there is a statistical time lag for the initial plasma channel to form, followed by a more repeatable exponential growth in the current, before the spark stabilizes [4], [9]. The quantity of material removed, and the cut quality, depends heavily on how long the spark burns before being extinguished (because this corresponds to the energy available to vaporize the workpiece metal) [5].

Our first thought was to continuously sample the gap voltage using the microcontroller's ADC to determine when to interrupt the spark current, but the STM32's 1µs sampling interval is too coarse when the spark should only last a few µs. The solution is to detect spark onset using a comparator on the gap voltage, start a microcontroller timer, and cut off the current when the timer elapses. The STM32's timer can run at the 72MHz system clock frequency allowing timing control with 15ns resolution.

5) Feasibility of pure water as the dielectric fluid: In industry, high-purity oils are sometimes used as the dielectric fluid for EDM work, but these can be messy, costly, and break down only at very high voltages [6]. Pure (deionized or distilled) water can be used as an alternative, and works well under conditions similar to the voltage and gap height outlined above [4].

Dielectric fluid needs to replace what was present in the narrow gap before the spark occurred in off-time between sparks, which is only around 50us [5]. We will need to experiment with the apparatus to determine the best pump and nozzle configuration to accomplish this.

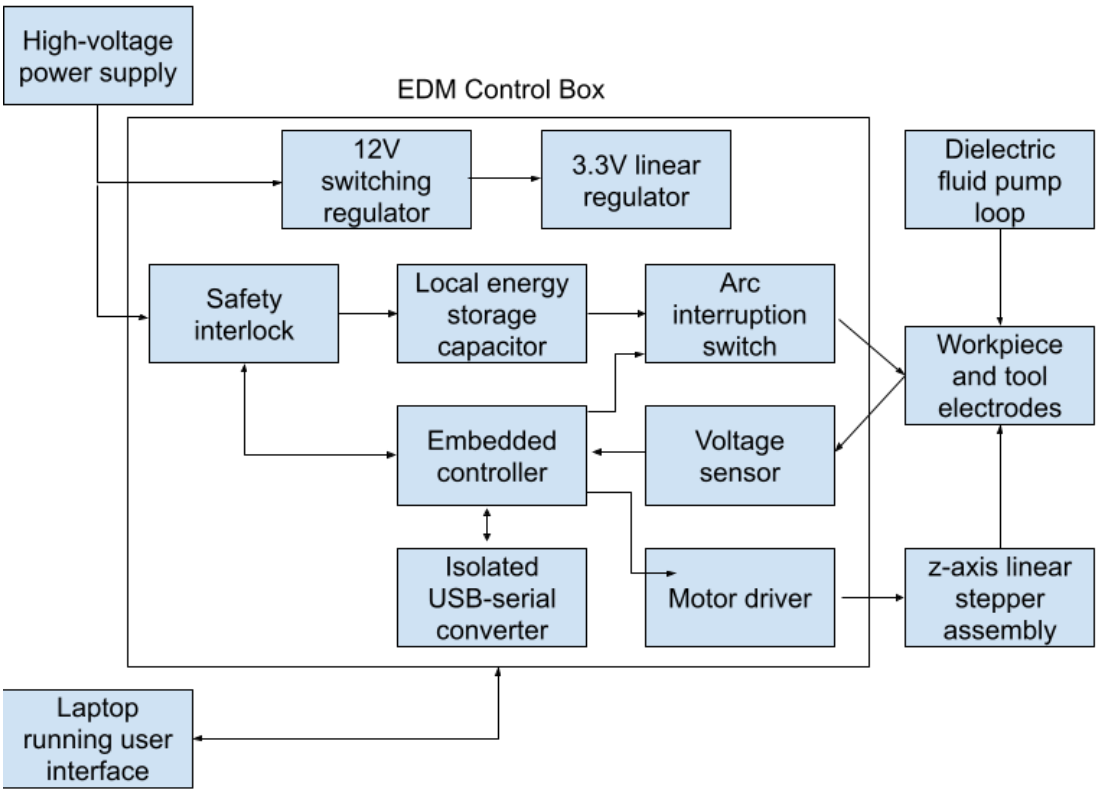

Fig. 13: Block diagram of the system

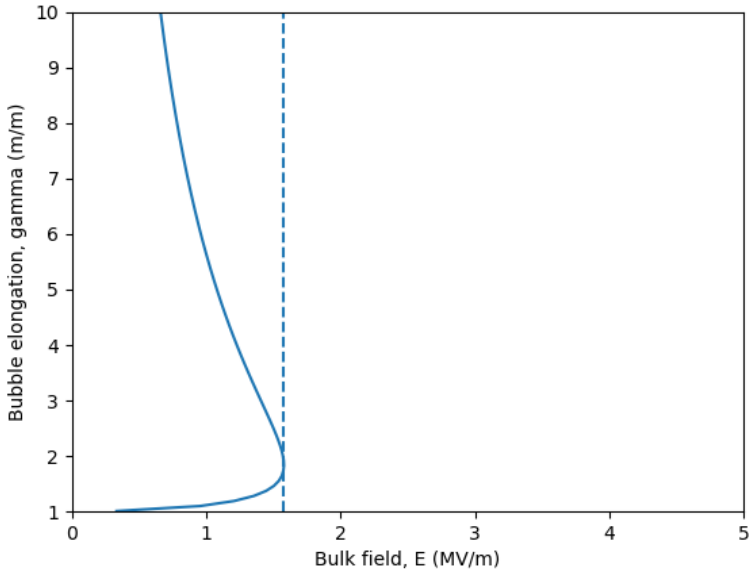

Fig. 14: A gas bubble in pure water elongates with increasing electric field (solid blue) up to the onset of instability at a critical field (dashed blue). The surface tension $\sigma = 74\mathrm{mJ/m^2}$ and relative permittivity $\epsilon = 81$ of pure water were used.

G. Major challenges

There are four major challenges that our group, The Cathode Blades, anticipates facing during the course of this project. The first challenge is the dangers posed by high voltage both to the project, and the engineers. High Voltages hold the potential to burn circuitry components, and melt hardware material so that the state of both is damaged and deformed beyond the point of repair to functionality. These voltages also pose a threat to users and engineers, as they can shock or burn those who handle them improperly. This often results in significant physical-injury to the victim of such an occurrence, and can incapacitate the person from continuing to use the product.

The second challenge is the complexity of the manufacturing process. EDM is a decently complicated process and consists of steps involving multiple parts that operate in a coordinative and sequential manner. All of these steps will not only need to work successfully on their own, in order for the operation to achieve its desired outcome, but they will also have to do so with precise timing in relation to one another. Managing the steps of this process all in conjunction with each other will create confusion, and possibly even unforeseen problems which will need to be addressed and overcome by the engineering team.

The third challenge involves coordination on the levels of programming and electric-signal connectivity. It will prove difficult to connect the user interface to the system of embedded hardware and firmware within the design of this project endeavor. This is because of all the complexities that are present in directing all of the controls, functions, and features to work together in accomplishing a common outcome. The completion of this task will require extensive attention and testing of numerous minute details. Any of these details has the potential to introduce error or obstacles into the team's progression towards the desired outcome.

The fourth challenge involves the coordination and spatial alignment of the moving hardware pieces that are included within this project. Managing all of these pieces to move in accordance with each other will be difficult in three-dimensional space the same way it will be difficult timewise. It will take extreme precision and accuracy to have everything align properly into place, so that necessary functions of the overall operation are able to occur as a result of different pieces working together.

H. Test plan

Before testing can proceed, we need to verify the three safety features of our device work as intended. First, the safety interlock switch should trip quickly in the event of an emergency stop input, a loss-of-signal from the PC, or a short of the output electrodes. When tripped, the safety interlock should de-energize the tool electrode and discharge the capacitor. Second, the z-axis limit switches, a loss-of-signal, or an e-stop should halt the z-axis motor drive. Third, we will verify that the optoisolator keeps the USB port connected to the control PC fully isolated from the voltages in our device, so that the operators never need to approach the device while it is powered.

At this point, we are safe to test the integrated system. We will remotely step the tool toward the workpiece until the gap is small enough that breakdown occurs repeatedly. During this time, we will observe the gap voltage waveform on the oscilloscope and compare it against the expected behavior. Each time the sparking stops, we will step the tool down to start it again. We hope to adjust the voltage level at which the spark detection comparator flips using a potentiometer so that while sparking, the MOSFETs alternate high and low, but a short is not detected by the ADC on the microcontroller. This way, the MOSFETs will control the sparking, but the safety interlock will not switch.

The final step is to configure the firmware for automated control of the z-axis and prepare for a final demonstration of a cut without operator intervention. This will be implemented through a state machine that automatically operates the motor during the machining process. Once this is done, we hope to quantify our design parameters.

I. Resources and equipment

We will make use of the hand and machine tools at Lacey hall, including the waterjet and laser cutting machines. We will need a power supply capable of delivering 100V at a few A continuously; a good supply is outside of our budget at this time.

J. Software tools

We will make use of the GNU x86-ARM cross-compiler and STM32 standard peripheral libraries to generate firmware binaries for the microcontroller, as well as the stlink-tools package to upload same. We will use the gdb debugging server to resolve software issues. We will use the AutoCAD software suite for mechanical drawings of components to be laser-cut and water-jetted, and the Multisim/Ultiboard programs for schematic capture and PCB artwork.

IX. Timeline

Starting off, the group met and established what the project involved, what basic equipment was required, and what general parts comprised the functioning of the EDM Machine. Roles and introductory tasks were delegated based upon skillset and knowledge from prior courses, as well as intellectual and curricular strengths.

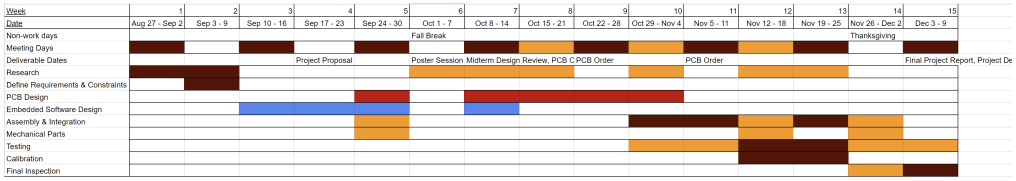

Fig. 15: Gantt chart - Tasks for Nathan are in blue, Hadrian are in red, Stephen are in green, and Everyone are in Brown

After establishing each member's roles, the group determined the concrete objectives that were aimed to be fulfilled by its EDM design. Plausible obstacles were then anticipated by the group, and concurrent work scheduling was arranged to account for these obstructions. The group recognized that the general tasks of circuit design, mechanical design, software programming, and part acquisition could all be completed in concurrence with each other. On the electrical front, the arc current, linear servo-drive, and power supply units were all figured out simultaneously by separate group members. In terms of the project's firmware side, the voltage sensor, servo motor, and microcontroller were also configured simultaneously. These three firmware aspects were developed collaboratively by different pair-combinations of group members. Even the external attachments to this project were formulated simultaneously by separate individuals of the group. The workpieces and tools, dielectric pump, and Z-axis mechanism for linear motion were all externally attached to the EDM's frame, and used in the act of arc channeling. These attachments were all gathered and incorporated into EDM function by different members of the group. The group then made its initial presentation, and began to uptake respective role-endeavors.

The first phase of the project occurred between the group's initial presentation and the submission of its project proposal. During this phase, the group began developing the elementary structure of the main parts to the EDM prototype. Hadrian designed the EDM machine's physical frame, envisioned the attachment to translate vertical motion into the discharge tool, and conceived the fundamental design of the connector piece within this attachment. Nathan developed the programming algorithm for instructing the spark cycle, and the necessary variables for processing cycle pulsation. Henry brainstormed the overall sectors of the EDM circuit. He then formulated the general subcomponents needed for implementing each of the sector functions. Stephen analyzed the constraints, requirements, and objectives of the dielectric pump. After this analysis, he researched and selected a fitting aquatic-pump for usage within the dielectric medium. Group members completed necessary, safety training with the workshop supervisor at Lacy Hall for subsequent use of power tools.

The second phase of the project occurred between the group's proposal submission, and its poster session. During this phase, the group evaluated which exact parts it would need to order, the costs and budgeting that corresponded to these parts, and acquiring parts on Grounds to save money. Hadrian initiated the ordering of parts, and then created a CAD design of the EDM machine's physical structure in three dimensions. Henry also diagrammed schematic designs for the machine's circuit-board sectors, establishing concrete subcomponent-configurations. He then constructed these schematics in KiCAD. Thirdly, he formed the team's block diagram to represent the overall control system for the EDM prototype. Nathan wrote basic code functions for the steps of EDM operation, and made sure that these functions involved the incoming parts in those steps. Lastly, Stephen carried out the beginning stage of searching for a power supply on Grounds. He did this by walking to SEAS laboratories, emailing lab supervisors and building directors, and searching pertinent university-websites.

The third phase of the project occurred between the group's poster session, and its midterm design review. In this phase, the group developed its PCB layout, its cycle-model technicalities, and its knowledge of power-supply availability on Grounds. Hadrian designed and constructed the PCB layout. Henry assisted the other group members with fulfilling their roles. He helped Stephen visualize a diagram and control system for the electric pump, and he helped Hadrian with the feasibility of the PCB layout design. Furthermore, he helped Nathan with three key aspects of programming the spark cycle. These aspects were the timing configuration of spark cycle stages, the exact sequence of steps that comprise the cycle, and these steps' correspondence to memory and hardware registers. Nathan programmed the set of code commands to carry out the cycle algorithm on the STM32 microcontroller, and enact spark cycling through the EDM machine. Stephen continued to search for a power supply, reaching contact with both the professor and graduate student who run UVA's EDM machine in the Materials Science Department. While there were no power supplies available to be borrowed from the university's EDM stockage, there was a fifty-volt power supply available for use in the workshop of Lacy Hall. No other labs or workshops outside of Capstone and Lacy were able to lend us a power supply, but the group had enough supply with the NI brick that it secured in the Capstone room to conduct preliminary analysis of microcontroller functioning. After these developments to the project were made, the group gathered to align each other's progress, and present our midterm design for review by the rest of the class.

The fourth phase of the project occurred between the group's midterm design review, and its PCB delivery. It involved completing the needed prerequisites for capability to initialize testing. Hadrian first completed the PCB design, and submitted it for order placement. He then had the attachment's connector piece cut to design specification with water-jetting assistance from Lacy Hall's supervisor. Henry verified the inclusion of necessary components and subcomponents to the finalized PCB design. This verification

was completed by ensuring the layout configuration was sufficiently viable for testing, spatial arrangement of soldered wires, and full functionality. He then assisted Nathan with coordinating the prototype's software program with its corresponding hardware operations. Nathan made preparations on the programming side by measuring the hardware's clock speed, voltage, motor movement, and time-pulsation width. Furthermore, he set up the analog-to-digital (ADC) converter for signal transmission in the prototype's (STM32) microcontroller board. Stephen completed the logistics of arranging for the team to undergo high-voltage safety training with UVA's Environmental Health and Safety (EHS) department. In order to accomplish this, he repeatedly corresponded with the EHS department's high-voltage safety supervisor, transferred needed project files from groupmates to the department, and coordinated a collectively available period for the group to undergo required training.

Key adjustments were made to each of the project's main areas as the development of the prototype progressed. Both the shaping of the connector piece, and the work tool's securing mechanism needed alteration after the piece was formed. This was because the channel breadth designed to fit into the servo motor's attachment-block was too narrow. Despite the precise measurement made of the block's height, which was used as a CAD specification during water-jetting, this breadth fell slightly short of this height. Additionally, the concave curvature of the spine hold for the C clamp did not fully fit the clamp's spine. Measurement errors could've possibly been made for this value and curve shape respectively, but the precision of these measurements leave minuscule inaccuracies of the jet cutter as the likely source of product error. Since the group couldn't attain a snug fitting of the clamp into the concave hold of the connector piece, the clamp mechanism for securing the work tool was scrapped. In order to sufficiently replace the clamp's tightness, a vertical hole was drilled through the connector piece at a slightly smaller diameter than the work tool. This tiny difference allowed for the tool to be threaded through the hole, with enough resistance to keep it tightly in place as the servo motor moved it along the machine's vertical axis.

On the electrical side of the group's project, there were many adjustments that needed to be made leading up to, and during testing. These adjustments were in the areas of microcontroller operation, microcontroller handling of voltage rails, short circuiting, component functioning when handling current, and signal detection.

After soldering down the STM32 microcontroller and supporting parts, we tried to connect the SWLink interface tool and flash firmware. This failed because we had routed the SWDIO and SWCLK debugger signals to the wrong microcontroller pins; greenwiring fixed the issue and we were able to flash firmware. When the microcontroller executed the first instruction (even if it was just a NOP) in its firmware binary, it tripped a HardFault exception and halted the processor. STM documentation suggested two possible causes: external oscillator instability, and supply rail fluctuations. When the microcontroller was configured to operate off the internal oscillator, the problem remained, ruling out the first possibility. Addressing the second possibility would require a board redesign to place decouplers next to to each of the microcontroller rail pins, which was not possible in the time remaining. The group ultimately chose to wire an STM32 breakout to our board to get the system up and running.

The 3.3V linear regulator that steps down the 12V rail to power the micrcontroller and a few other ICs on the board also gave us difficulties. At first, this regulator worked alright, but had a lot of noise on the output (200mV near 10kHz), probably to the low-ESR output decoupler being far away. Soldering another decoupler right across the output fixed this issue, and we proceeded with initial bringup of the microcontroller. After a certain point, the regulator began to short the 12V rail. Desoldering the part allowed us to measure that the input pins were Zener-shorted above 1.8V, and the output pins were shorted whenever the part was warm. Since we didn't have a replacement part and weren't sure of the failure mode, we decided to power the 3.3V rail from the STM32 breakout's regulator (ultimately, this draws power from a USB port and linear regulator).

At this point, we had a microcontroller installed and a solution to power both the 3.3V and 12V rails separately. Unfortunately, the 12V rail was now shorted. To find the short, we placed the negative and positive leads of a millivolt-meter at the input connector GND and 12V, respectively, and directed 10mA around the short circuit. We then moved the negative lead along the GND net up the potential gradient and the positive lead along the 12V net down the potential gradient, expecting that the potentials would come together approaching the short. We found that the push-pull gate driver for the FET spark switch had continuous shoot-through current. The gate driver has a serious design flaw in the interface between the single-ended 3.3V-12V level shifter and the push-pull pair which causes both transistors in the pair to enter saturation. Without a board redesign, all we could do was eliminate the push-pull pair and drive the FET gates directly from the single-ended level shifter. This was accomplished by desoldering the push-pull transistors and installing a single jumper.

The BJT driver collector resistor now limited the current charging the FET gate capacitance, raising the switch-on time to an unacceptable level 10us. To resolve this, we reduced the collector resistance from 1k to 180; we had to also reduce the b-e junction current limiter from 1k to 220 to raise the base current since the transistor beta was pretty low, 50x.

We experienced difficulty sixteenth-stepping the z-axis motor. In the prototyping stage, we only operated the driver at full steps, but sixteenth steps require a steady-state holding current through the motor coils, and we had to learn to adjust the A4988 stepper driver to an appropriate current level sufficient to move the rotor without heating the coils too much.

We experienced an issue after including the state machine in the code where the microcontroller would HardFault partway through the first state machine loop. Using gdb, we were only able to examine the stack register to determine that this was an Undefined

Instruction error occuring at a program counter location corresponding to the function calc(underscore)voltage(underscore)avg(). The function was just three lines of code, so Henry changed things until the error disappeared instead of trying to figure out the error. It turned out that the total variable used to calculate the average needed to be declared as volatile for some reason in order for the add-in-place ARM instruction to be valid. Probably a compiler bug.

The RX and TX LEDs did not illuminate when the USB virtual serial port transceived bytes because we forgot to route the LED cathodes to the open-drain pins of the USB-serial converter IC. Green-wiring these connections fixed the issue. The comparator output behaved the opposite of how we interpreted the datasheet. Since it was an open-collector output, only the falling edge was fast, and we wanted to associate this with a falling gap voltage to quickly detect spark onset. We greenwired to commute pins 2 and 3 to fix this mistake. The UART optisolator circuit had two design flaws. First, the circuit inverted the RX and TX signals. We fixed this by reconfiguring the FTDI USB-UART converter to invert RX and TX a second time so as to hide this mistake from the microcontroller. Second, the phototransistor side of the optoisolator showed a very slow rise time (time constant 10ms). This was because we had tried to decouple the base capacitance to ground with a capacitor as recommended in the datasheet for analog coupling applications. For a high-speed digital application, the decoupling is not appropriate so we cut the capacitor.

X. Costs

Most of the costs associated with this project come from our budget of 500 dollars that was given to us by the University of Virginia. From this budget, our total costs were $319.57. The full breakdown of all parts ordered and their price can acessed through the spreadsheet linked below.

https://docs.google.com/spreadsheets/d/1gkj42s6W9cKnPwbhNErwmk3UejOko-4D/edit?usp=sharing&ouid=108773830560211227509&rtpof=true&sd=true

In addition, many of our costs come from orders made personally by our group members. The total costs from these orders are $199.69. The recipts for these orders can be found below. A simplified table can also be found in the appendix.

https://drive.google.com/drive/folders/1NdhwiNCfO2ydW88enpjz_QD7k1ebqeML?usp=sharing

This brings are grand total costs to $519.26. It is likely that if our product were to be produced at a larger scale, the costs would be under $500, but due to the nature of our product, it would be difficult to mass produce our device.

XI. Final Results

Our team solved the engineering problems of building an EDM system, but not the physics problems: we were able to build a device that meets all the requirements we originally decided on, but those requirements did not make for a system that could achieve the project objectives.

During PCB bring-up, which started in the last two weeks of the project, we faced a series of difficulties (see Timeline) in both hardware and software, and were able to overcome these one after another until we had our board and PC control program working together as intended. We got all of these parts of the project working:

- z-axis stepper motor control
- safety interlock relay control
- short detection and prompt shutoff response
- PC control program readout of gap voltage and FSM state
- spark detection and precision timing of spark duration
- gap voltage measurement synchronous with sparks
- FSM control via the PC program
- control loop with z-axis motor as the output and average spark-synchronous gap voltage as the input
- FETs spend minimal time between cutoff and saturation and are not damaged by spark current

Unfortunately, we were not able to achieve the main project objective, cutting into a block of metal using the EDM process. In each test we ran, the control loop moved the tool slowly down toward the workpiece (as expected, since no sparks were occuring and the gap voltage was above the controller setpoint). No sparks occurred until the tool made physical contact with the workpiece, at which point the short-detection code subsystem sent the FSM into the STOP state and ended the cut.

There is only one reason left for why our device does not generate sparks before electrode contact: the gap E-field is too weak to break down the water and form a plasma channel. To increase E, we either have to raise the gap voltage or bring the electrodes closer together. Raising the gap voltage would require us to purchase a high-voltage high-current power supply outside our budget and redesign the FET switch to withstand higher voltages. Bringing the electrodes closer together without them touching would require sourcing a finer-pitch lead screw assembly and building a more rigid mechanical assembly (we noticed small transient ”bouncing” of the tool after each motor step).

XII. Future Work

Future work for this project would be to continue testing the device that has been built and to develop it so that it is able to cut all the way through a piece of metal. This project only has movement in the z-axis, another feature that could be added in the future is to give it movement in the x and y directions. This could be done by either moving the copper tool piece or alternatively by

moving the work piece. Other improvement includes, building a case to hold the entire device, cleaning up the PCB, and integrating the user interface into the embedded code. The current project is split into three different pieces and it would be better to have all three of these pieces held by one case. The current project has had to rewire some parts of the PCB, therefore, future work could include reworking the PCB design some so that the STM32 chip on the PCB works. A UI has been coded but time constraints have prevented the UI from being integrated into the embedded code. With more time, all of these issues could be fixed relatively easily.

For others wanting to reproduce this project, it would be advised to setup the embedded peripherals quickly because that caused more troubles than expected. Also, routing the PCB took longer than expected, so starting on that early would be recommended. The team had some difficulties finding a power supply that could reach the optimum voltage, therefore, finding a 100 V power supply could greatly help a future team working on this project. Before starting this project, it seemed as though drilling through a piece of metal would be achievable with a 100 V power supply. However, after testing the project, it seems that 100 V may not be large enough. Future groups wanting to work on this project should use a larger voltage.

REFERENCES

[1] L. Bass, P. Clements, and R. Kazman, Electric discharge hybrid-machining processes : fundamentals and applications First edition. [E-book] Available: PDF https://doi.org/10.1201/9781003202301

[2] D. Huzel and D. Huang, Modern Engineering for Design of Liquid-Propellant Rocket Engines. [E-book] Availavle: Google Books

[3] C. Percival, "Engine Cooling – Why Rocket Engines Don't Melt" everydayastronaut.com, Jan. 13 2022. [Online]. Available: https://everydayastronaut.com/engine-cooling-methodes/

[4] C. Raza, C. K. Nirala, "Multiphysics simulation of plasma channel formation during micro-electrical discharge machining" AIP Advances, vol. 11, 2021. https://pubs.aip.org/aip/adv/article/11/2/025138/966594/Multiphysics-simulation-of-plasma-channel

[5] E. Weingärtner, F. Kuster, K. Wegener, "Modeling and simulation of electrical discharge machining" Procedia CIRP, vol. 2, pp. 74-78, 2012 https://www.sciencedirect.com/science/article/pii/S2212827112001448

[6] D. K. Chung, B. H. Kim and C. N. Chu, "Micro electrical discharge milling using deionized water as a dielectric fluid", Journal of Micromechanics and Microengineering, vol. 17, no. 5, March 2007 https://iopscience.iop.org/article/10.1088/0960-1317/17/5/004

[7] M. Szklarczyk, R. C. Kainthla and J. O. Bockris, "On the Dielectric Breakdown of Water: An Electrochemical Approach", Journal of The Electrochemical Society, vol. 136, no. 9, 1989 https://iopscience.iop.org/article/10.1149/1.2097451

[8] T. Kitamura, M. Kunieda, K. Abe, "Observation of relationship between bubbles and discharge locations in EDM using transparent electrodes", Precision Engineering, vol. 40, pp. 6-32, April 2015 https://www.sciencedirect.com/science/article/abs/pii/S014163591400155X?via

[9] S. M. Korobeynikov, Y. N. Sinikh, "Bubbles and breakdown of liquid dielectrics", IEEE Xplore, June 1998 https://ieeexplore.ieee.org/document/694865

[10] C. G. Garton, Z. Krasucki, " Bubbles in Insulating Liquids: Stability in an Electric Field", Proceedings of the Royal Society of London. Series A, Mathematical and Physical Sciences, vol. 280, no. 1381, July 1964 https://www.jstor.org/stable/2414907

[11] Z. Li, H. Li, F. Lin, Y. Chen, D. Liu, B. Wang, H. Li, Q. Zhang, "Lifetime investigation and prediction of metallized polypropylene film capacitors", Microelectronics Reliability, vol. 53, no 12, pp. 1962-1967, December 2013 https://www.sciencedirect.com/science/article/abs/pii/S0026271413001571

[12] Polypropylene Pulse/High Frequency Capacitors, "R75, Single Metallized Polypropylene Film, Radial, DC and Pulse Applications (Automotive Grade)", KEMET Electronics Corporation, September 2023 https://connect.kemet.com:7667/gateway/IntelliData-ComponentDocumentation/1.0/download/datasheet/R75IR51004040J

[13] "Mainstream Performance line, Arm Cortex-M3 MCU with 64 Kbytes of Flash memory, 72 MHz CPU, motor control, USB and CAN", STMicroelectronics, 2023 https://www.st.com/en/microcontrollers-microprocessors/stm32f103c8.html

[14] "§ 15.5 General conditions of operation.", Code of Federal Regulation, 13 October 2010 https://www.ecfr.gov/current/title-47/chapter-I/subchapter-A/part-15/subpart-A/section-15.5

[15] "§ 15.101 Equipment authorization of unintentional radiators.", Code of Federal Regulation, 2 November 2017 https://www.ecfr.gov/current/title-47/chapter-I/subchapter-A/part-15/subpart-B

[16] "2100 ELECTRICAL SAFETY PROGRAM", University of Virginia Facilities Management, 13 May 2016 https://www.fm.virginia.edu/docs/ohs/ElectricalSafetyProgram.pdf

[17] "Features of IPC 7351 Standards to Design a PCB Component Footprint", Sierra Circuits Proto Express, 7 December 2022 https://www.protoexpress.com/blog/features-of-ipc-7351-standards-to-design-pcb-component-footprint/

[18] "Trace Spacing: A Guide For PCB Design", JHDPCB, n.d. https://jhdpcb.com/blog/trace-spacing-design

[19] Mitsuharu Onodera Kaoru Onodera Kaoru Hiraga Hiraga, inventor; FANUC Corp, assignee. Wire electrical discharge machine for machining while adjusting machining conditions. Japan patent JP6140228B2. 27 August 2015

[20] Fabio Nogueira Leao, Alexander Xidacis, Martyn CUTTELL, Inventor; Rolls Royce PLC, assignee. Electrical discharge machining. US patent US9707637B2. 18 July 2017

[21] Lin Gu, Guojian He, Inventor; Shanghai Jiaotong University, assignee. Multifunctional Integrated Manufacturing System Based On Electrical Arc And Discharge Machining. US Patent US20200238414A1. 22 January 2020

XIII. APPENDIX

TABLE I: Table 1: Simplified Budget Costs

Index	Manufacturer Part #	Qty in Stock	Qty Req'd	Per Unit Price	Cost	Team Name	Comments
1	3177T13	Not Listed	1	$6.93	$6.93	Cathode Blades	
2	8966K731	Not Listed	3	$4.08	12.24	Cathode Blades	
3	91735A199	Not Listed	1	$5.55	5.55	Cathode Blades	
4	90257A009	Not Listed	1	$8.65	8.65	Cathode Blades	
5	90107A010	Not Listed	1	$4.11	4.11	Cathode Blades	
6	15275A57	Not Listed	3	$2.69	$8.07	Cathode Blades	
7	moib-1875	Not Listed	1	$9.88	9.88	Cathode Blades	
8	332-CC-20YD-6BN	Not Listed	1	$7.20	7.2	Cathode Blades	
10	B32928A4206K000	128	2	$29.66	59.32	Cathode Blades	
11	8619K481	Not Listed	1	$24.15	24.15	Cathode Blades	
12	5233K67	Not Listed	1	$10.60	10.6	Cathode Blades	10 ft.
13	4387T51	Not Listed	1	$10.23	10.23	Cathode Blades	
14	6184A43	Not Listed	1	$12.89	12.89	Cathode Blades	
15	R75IR51004040J	78	1	$9.80	9.8	Cathode Blades	
16	ASTM32F103C8T6	Not Listed	1	$12.88	12.88	Cathode Blades	Cannot Buy Through other Vendors
17	WWZMDiB	Not Listed	1	$7.99	7.99	Cathode Blades	Cannot Buy Through other Vendors
18	17HE08-1004S	Not Listed	1	$8.99	8.99	Cathode Blades	Less than 1/5 the price of McMaster
19	FR-PPU12-10	Not Listed	1	$19.99	19.99	Cathode Blades	Less than 1/5 the price of McMaster
20	CF14JT1K00		17	0.056	0.952	CathodeBlades	
21	PN2907ABU		5	0.34	1.7	CathodeBlades	
22	CF14JT10K0CT-ND		29	0.04	1.16	CathodeBlades	
23	490-9139-1-ND		29	0.284	8.236	CathodeBlades	
24	4878-2N2222ACT-ND		9	0.16	1.44	CathodeBlades	
25	490-9077-1-ND		5	0.43	2.15	CathodeBlades	
26	CF14JT100RCT-ND		3	0.1	0.3	CathodeBlades	
27	CF14JT10R0CT-ND		5	0.1	0.5	CathodeBlades	
28	CTX917-ND		3	0.25	0.75	CathodeBlades	
29	277-1260-ND		5	2.44	12.2	CathodeBlades	
30	497-6063-ND		3	6.42	19.26	CathodeBlades	
31	160-1300-5-ND		5	0.44	2.2	CathodeBlades	
32	609-4050-1-ND		3	0.77	2.31	CathodeBlades	
33	296-6609-5-ND		3	0.48	1.44	CathodeBlades	
34	1727-BZX79-C3V0,143CT-ND		3	0.16	0.48	CathodeBlades	
35	Z2834-ND		3	3.54	10.62	CathodeBlades	
36	895-FT232RNL-REEL		3	4.8	14.4	CathodeBlades	PCB
	Total Costs:						